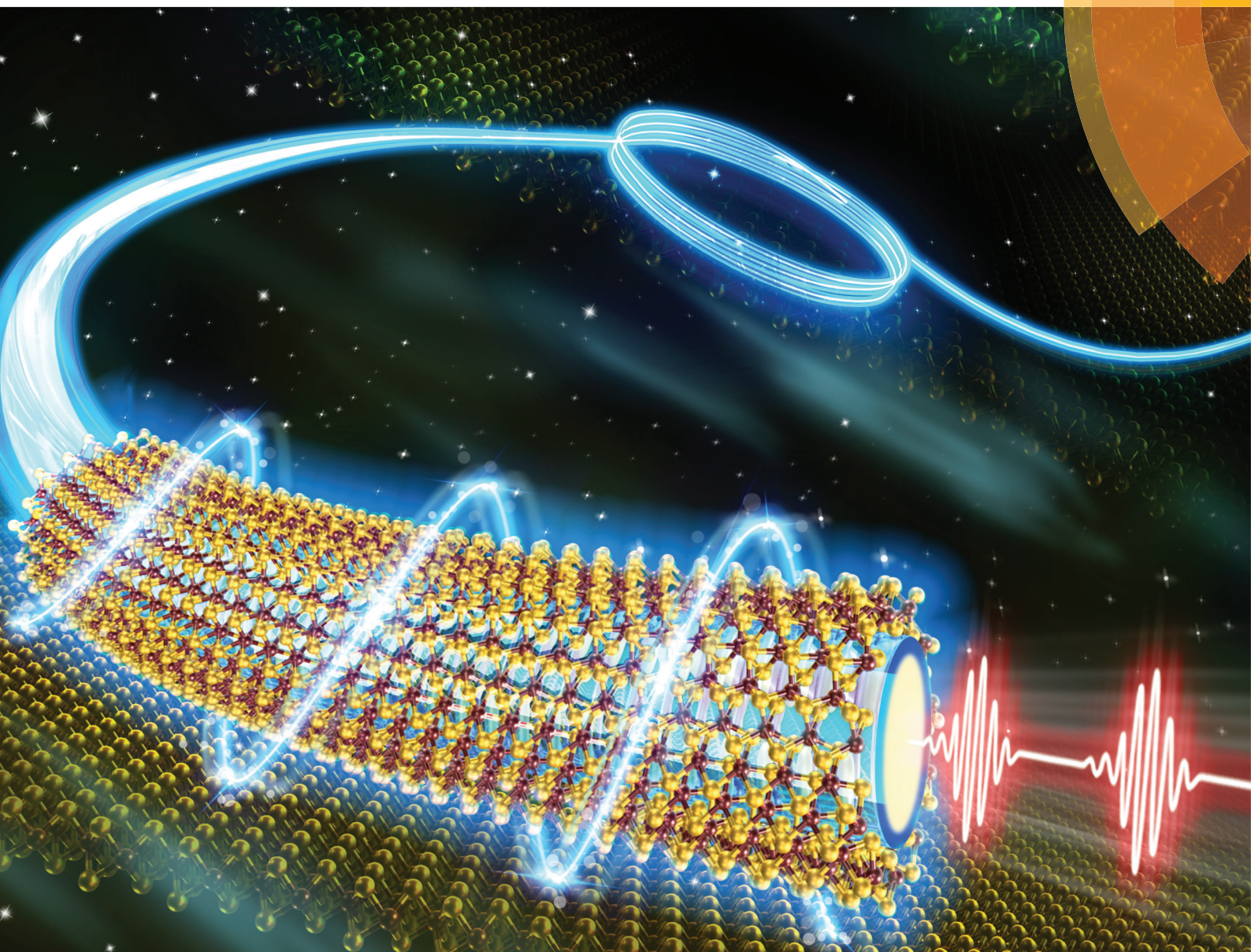


Nanoscale

rsc.li/nanoscale



ISSN 2040-3372



PAPER

Ming Lei, Zhiyi Wei *et al.*

Tungsten disulphide for ultrashort pulse generation in all-fiber lasers



Cite this: *Nanoscale*, 2017, 9, 5806

Tungsten disulphide for ultrashort pulse generation in all-fiber lasers

Wenjun Liu,^{a,b} Lihui Pang,^b Hainian Han,^b Ke Bi,^a Ming Lei^{*a} and Zhiyi Wei^{*b}

Tungsten disulphide (WS₂), which exhibits excellent saturable absorption properties, has attracted much attention in the applications of photonic devices. In this paper, WS₂ is applied for the preparation of a saturable absorber (SA). Using the pulsed laser deposition (PLD) method, WS₂ is deposited on the side surface of the tapered fiber. In order to obtain larger non-linearity of the SAs with evanescent wave interaction, the tapered fiber had a smaller waist diameter and longer fused zone. Gold film was deposited on the fiber-taper WS₂ SAs to improve their reliability and avoid oxidation and corrosion. Employing the balanced twin-detector method, the modulation depth of the fiber-taper WS₂ SAs was measured to be 17.2%. With the fiber-taper WS₂ SA, a generated pulse with 246 fs duration and a 57 nm bandwidth was obtained at 1561 nm. The electrical signal to noise ratio was better than 92 dB. To our knowledge, the pulse duration was the shortest among the reported all-fiber lasers with transition metal dichalcogenide (TMD) SAs. These results indicate that fiber-taper WS₂ SAs with smaller waist diameter and longer fused zone are promising photonic devices for ultrashort pulse generation in all-fiber lasers.

Received 9th February 2017,
Accepted 27th February 2017

DOI: 10.1039/c7nr00971b

rsc.li/nanoscale

1 Introduction

As typical two-dimensional (2D) materials, transition metal dichalcogenides (TMDs) have been the objects of extensive theoretical and experimental studies due to their nice features in the development of new photonic devices.^{1–7} On the other hand, ultrashort pulse all-fiber lasers have characteristics such as high peak power, high pulse energy and low thermal effects, and they have broad applications in fields such as ultrafast optics, optical communications, non-linear optics and industrial processing.^{8–11} Recently, all-fiber lasers based on TMD materials have drawn great interest due to their outstanding advantages in generating ultrashort pulses.^{12–14}

In all-fiber lasers, the pulse output can be realized through Q-switching or mode-locking technology.¹⁵ The saturable absorber (SA) is the critical optical component of these all-fiber lasers, and the saturable absorption materials used for SAs should have wide optical bandwidth, fast response time and low loss properties. Additionally, in order to get ultrashort pulses, the modulation depth and damage threshold of the SAs should be considered.¹⁴ Semiconductor saturable absorber mirrors (SESAMs), which have limitations such as relatively narrow operation bandwidths, and complex and costly fabrica-

tion processes, have been considered as one kind of mode-locking component.^{16,17} With the development of material technology, single-wall carbon nanotubes (SWCNTs) and 2D materials, such as graphene, topological insulators (TIs) and TMDs, have been used as SA materials, and the SAs based on these materials have been studied for the generation of ultrashort pulses.^{18–29} Although SWCNT SAs have the advantages of low cost and easy integration,^{18–20} they require complex operating procedures to work in a specific wavelength.^{21,22} Graphene SAs (GSAs) with wide band absorption, ultrafast recovery time and strong non-linearity can be used to overcome the disadvantages of SWCNT SAs,^{23–25} but the relatively weak light absorption coefficient and zero band gap features have limited their applications in optoelectronic devices.²⁶ TIs have a large modulation depth and saturable intensity, but the indirect band gap of TIs is not conducive to their optoelectronic applications.²⁶ TMDs have been successfully applied to the preparation of SAs due to their non-zero band gap and layer-dependent second-order optical non-linearity properties.^{14,27} By controlling the thickness or atomic defects, SAs based on TMDs have the advantage of ultrafast carrier dynamics, high third-order non-linear susceptibility and broadband saturable absorption,¹⁴ and they have been widely used in all-fiber lasers.^{28,29}

Q-switched fiber lasers based on molybdenum disulfide (MoS₂) have been reported,^{30–33} and mode-locked fiber lasers have been experimentally demonstrated around 1030 nm, 1550 nm and 2000 nm.^{34–37} Dual-wavelength domain-wall dark pulses have also been obtained.³⁸ For tungsten disulphide

^aState Key Laboratory of Information Photonics and Optical Communications, School of Science, P. O. Box 91, Beijing University of Posts and Telecommunications, Beijing 100876, China. E-mail: mlei@bupt.edu.cn

^bBeijing National Laboratory for Condensed Matter Physics, Institute of Physics, Chinese Academy of Sciences, Beijing 100190, China. E-mail: zywei@iphy.ac.cn

(WS₂) SAs, the Q-switched and mode-locked operations have also been achieved.^{39–49} On the other hand, in order to realize the high power tolerance and long interaction length of SAs, and also the evanescent wave interaction of the 2D materials, the layer has been used with a side-polished fiber or tapered fiber.^{50–56} However, the shortest mode-locked pulse duration of all-fiber lasers based on a WS₂ SA is only about 595 fs,³⁹ which is wider than those in other 2D material SA fiber lasers. Thus, it is necessary to optimize the performance of the WS₂ SA with evanescent wave interaction, and further narrow the pulse duration in WS₂ SA fiber lasers.

In this paper, an all-fiber mode-locked erbium-doped fiber (EDF) laser, based on a WS₂ SA with evanescent wave interaction, is presented with a 246 fs pulse duration, which is the shortest mode-locked pulse generated from an all-fiber laser based on TMD material SAs. The WS₂ will be deposited on the tapered fiber by the pulsed laser deposition (PLD) method, and the fiber-taper WS₂ SA will be prepared. In order to obtain the larger non-linearity of SAs, the tapered fiber has a smaller waist diameter and longer fused zone. Following the preparation of the fiber-taper WS₂ SA, the gold film will be deposited on the surface to improve the reliability and avoid oxidation.

2 Fabrication and characterization of fiber-taper WS₂ SA

The details of the preparation process for the fiber-taper WS₂ SA can be seen in our previous work.¹⁵ Different from other works, the waist diameter of the fiber-taper WS₂ SA with evanescent wave interaction is only about 13 μm , and the effective length of the fused zone is about 4 mm (Fujikura FSM-100P). When the waist diameter of the fiber-taper WS₂ SA is smaller, and the effective length of the fused zone is longer, the non-linearity of the WS₂ SA will be stronger. Thus, the non-linear characteristics of the WS₂ SA can be controlled, and the modulation depth of the WS₂ SA can be increased. The scanning electron microscopy (SEM) image of the fiber-taper WS₂ SA is shown in Fig. 1(a). With the PLD method, WS₂ grown on the side surface of the tapered fibre has a purity of 99.8%. The vacuum degree is set at 6×10^{-6} mbar, and the 2 mJ per pulse laser beam is emitted from a Nd:YAG laser (SL II-10, Surelite). The time of deposition is about 3 hours, and the temperature of deposition is set to room temperature. Following this, the gold film is deposited on the SA layer. The time of deposition is about 30 minutes, and the thickness is about 180 nm. The gold film coated on the SA layer can be used to isolate the inner SA layer and avoid oxidation and corrosion by the environment. The larger scale microscopic image of the fiber-taper WS₂ SA can be seen in Fig. 1(b). The Raman spectrum in Fig. 1(c) confirms that the WS₂ element is being deposited on the tapered fiber. As seen in Fig. 1(d), using the balanced twin-detector method, the modulation depth of the fiber-taper WS₂ SA is shown to be approximately 17.2%, the saturation intensity is 34.02 MW cm⁻², and the non-saturable loss is 59.5%.

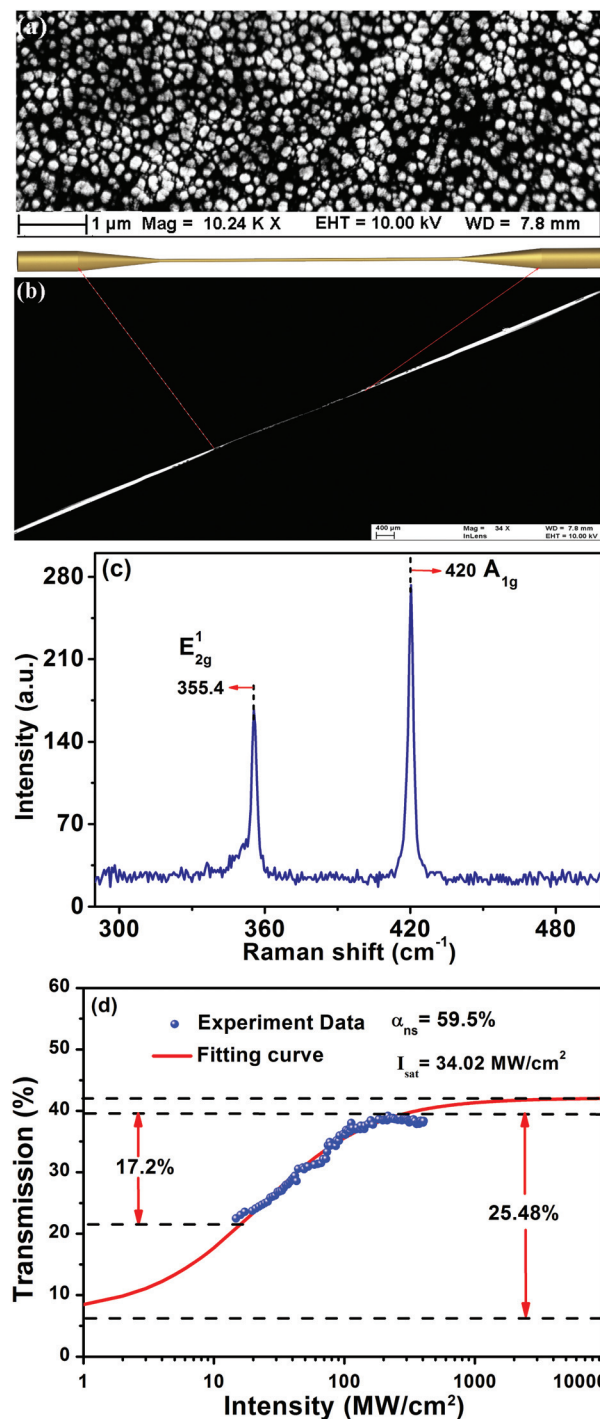


Fig. 1 (a) SEM image of the fiber-taper WS₂ SA. (b) Larger scale microscopic image of the fiber-taper WS₂ SA. (c) Raman spectrum of the deposited WS₂ on the fiber-taper SA. The two optical phonon modes are at 355.4 cm⁻¹ and 420 cm⁻¹. (d) Non-linear saturable absorption of the fiber-taper WS₂ SA. The modulation depth is approximately 17.2%, the saturation intensity is 34.02 MW cm⁻², and the non-saturable loss is approximately 59.5%.

The pulse source for measuring the modulation depth is a home-made fiber laser with a 1550 nm centre wavelength, 80 MHz repetition rate and 200 fs pulse duration. The modu-

lation depth is relatively high. In addition to the excellent optical properties of WS_2 , the high modulation depth is also due to the long effective length of the fused zone and compact coating of WS_2 on the tapered fiber. The long fused zone will lead to full interaction between the evanescent wave and WS_2 , resulting in an increase in the modulation depth of the SA. When using the PLD method, the WS_2 deposited on the tapered fiber is very compact and robust. This method can increase the contact area between the fused zone and WS_2 , as well as enhance the interaction strength between the evanescent wave and WS_2 . As a result, the modulation ability on the light can be increased. Another home-made fiber laser with 27 mW output power (about 243 mW in the WS_2 SA) and 100 MHz repetition rate has been used to measure the damage threshold of the WS_2 SA. The output pulse energy is about 2.43 nJ, and the damage threshold is measured to be about 309 mJ cm^{-2} .

3 Setup of passively mode-locked EDF lasers based on the fiber-taper WS_2 SA

The schematic diagram of our fiber laser, based on the fiber-taper WS_2 SA with evanescent wave interaction, can be seen in Fig. 2. The prepared fiber-taper WS_2 SA is incorporated into the all-fiber laser between the wavelength division multiplexer (WDM) and polarization controller (PC). The fiber laser is pumped by the 976 nm laser diode (LD) via a fused 980/1550 nm WDM. The single-mode optical fiber (SMF) in the cavity is the 1.25 m SMF-28 fiber ($-22 \text{ fs}^2 \text{ mm}^{-1}$). The EDF is the Liekki 110-4/125 fiber with a length of 62 cm ($12 \text{ fs}^2 \text{ mm}^{-1}$). Due to the hybrid structure composed of the tapered fiber, the WS_2 film and the gold film, the dispersion of the WS_2 SA could not be accurately calculated. Thus, the net dispersion for this all-fiber laser could not be accurately obtained. The mode-locked pulse is output by a 10 : 90 optical coupler (OC). The maximum output power from the OC is 18 mW with 680 mW pump power. Two PCs were used to

change the polarization states of the optical fibers in the ring cavity. The polarization independent isolator (PI-ISO) is incorporated to guarantee the single-direction operation. The output pulses from the 10% output OC are measured by an optical spectrum analyzer (Yokogawa AQ6315A), RF spectrum analyzer (ROHDE & SCHWARZ FSW26), and an optical intensity autocorrelator (Femtochrome, FR-103XL).

As shown in Fig. 3(a), based on the fiber-taper WS_2 SA with evanescent wave interaction, the EDF laser can be mode-locked at 1561 nm. When we open the pump source, the pulses in the fiber laser pass through the fiber-taper WS_2 SA, and the evanescent waves are generated in the fused zone of the tapered fiber. With an increase in the pump power, the intensity of the evanescent wave is enhanced, the non-linear phase shift decreases, and the saturated absorption of the WS_2 SA starts based on the evanescent wave interaction. When the peak pulse power is close to the saturation intensity of WS_2 , the absorption of WS_2 becomes the non-linear attractive effect. At this time, the non-linearity of WS_2 is evident: for the irregular pulse, the strongest pulse prioritises the absorber bleaching, and the pulse intensity increases rapidly. Due to the further amplification of the strongest pulse, which occupies a

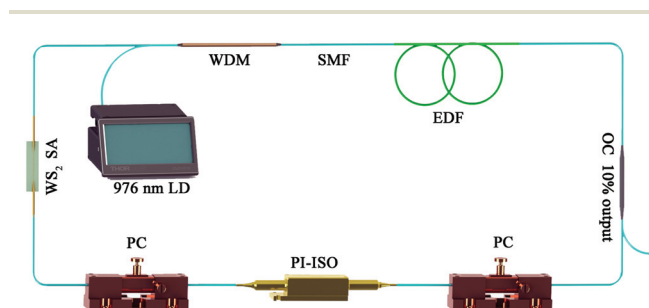


Fig. 2 Schematic diagram of the all-fiber mode-locked EDF laser based on the fiber-taper WS_2 SA. LD: laser diode; WDM: wavelength division multiplexer; SMF: single-mode optical fiber; EDF: erbium-doped fiber; OC: optical coupler; PC: polarization controller; PI-ISO: polarization independent isolator; WS_2 SA: fiber-taper tungsten disulphide saturable absorber.

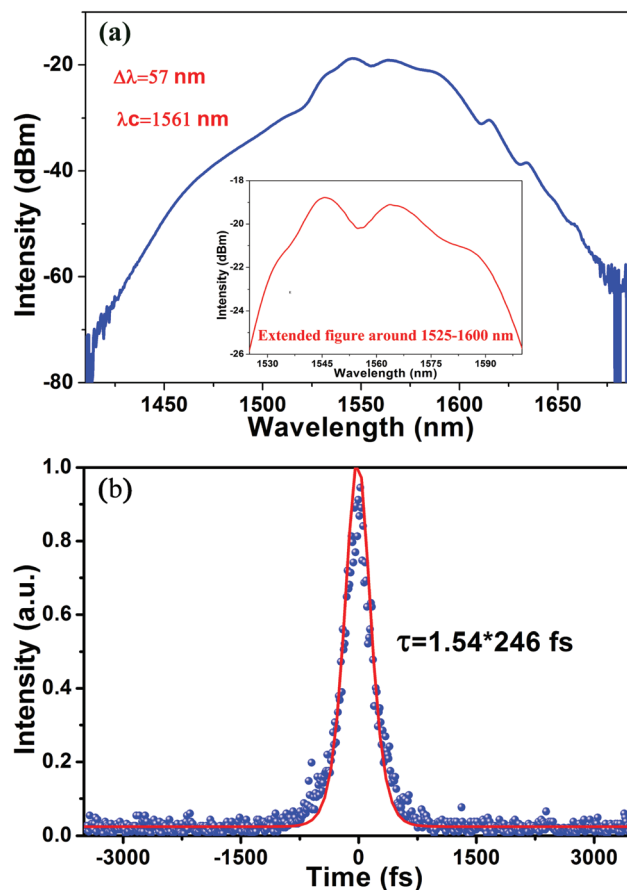


Fig. 3 Experimental results of the all-fiber mode-locked EDF laser based on the fiber-taper WS_2 SA. (a) Optical spectrum of the generated pulses. The 3 dB spectral width is about 57 nm at 1561 nm. (b) Intensity autocorrelation trace with 246 fs pulse duration.

large portion of the gain, the weak pulses are suppressed and weakened due to the absorption effect of WS_2 . Thus, the pulses will be compressed after they pass through the WS_2 SA. After repeated circular reactions in the ring cavity of the fiber lasers, the initial pulse is compressed and narrowed, and finally the stable mode-locking pulse is formed. The mode locking is aided by a greater modulation depth. The 3 dB spectral width of the mode-locked pulse is about 57 nm. With an optical intensity autocorrelator, the pulse duration is measured to be 246 fs in Fig. 3(b).

When the pump power is 680 mW, the maximum output power of the fiber laser is 18 mW, which is relatively high. The WS_2 SA has a high power tolerance. Before reaching the damage threshold, the WS_2 SA can enhance the non-linearity of the cavity, reduce the mode-locked threshold, and realize mode-locking faster. Moreover, the effective length of the fused zone is long, and the WS_2 deposited on the tapered fiber is compact and robust. The contact area between the fused zone and WS_2 is large, which is more conducive to heat dissipation. All of these reasons can explain the increase of the cavity power of the fiber laser.

The repetition rate is about 101.4 MHz, and the electrical signal to noise ratio (SNR) is better than 92 dB, and these are both measured with 30 Hz resolution bandwidth (RBW) as shown in Fig. 4. The 92 dB SNR means that the EDF laser is mode-locked stably. The phase noise of the fiber laser is also

Table 1 Comparison of mode-locked EDF lasers based on different TMD SAs. PD is the pulse duration, SNR is the signal to noise ratio, SW is the spectral width, and MD is the modulation depth

| TMDs | PD (fs) | SNR (dB) | SW (nm) | MD (%) | Ref. |
|-----------------|---------|----------|---------|--------|-----------|
| MoS_2 | 606 | 97 | 6.1 | 2.7 | 36 |
| MoSe_2 | 1090 | — | 2.3 | 1.4 | 13 |
| WSe_2 | 1250 | — | 2.1 | 0.5 | 13 |
| WS_2 | 595 | 75 | 5.2 | 2.9 | 39 |
| WS_2 | 246 | 92 | 57 | 17.2 | This work |

Table 2 Comparison of mode-locked EDF lasers based on graphene and carbon nanotubes. AOP is the average output power

| Types of SAs | PD (fs) | SNR (dB) | SW (nm) | MD (%) | AOP (mW) | Ref. |
|------------------|---------|----------|---------|--------|----------|-----------|
| SWCNT SA | 110 | 70 | 41 | 10 | 8 | 50 |
| GSA | 124 | 65 | 48 | 11 | 1.5 | 51 |
| WS_2 SA | 246 | 92 | 57 | 17.2 | 18 | This work |

measured. From Fig. 4(b), we can calculate that the timing jitter is about 10 ps integrated from 1 MHz down to 10 Hz. The high SNR can be explained by the gold film being deposited on the surface of the WS_2 SA to prevent the fiber breaking and avoid oxidation and corrosion by the environment. Moreover, the compact coating of the WS_2 and gold film on the tapered fiber can reduce the influence of the environment on the all fiber laser.

Compared with the previous works based on TMD SAs, we found that the all-fiber mode-locked EDF laser in this paper, based on the fiber-taper WS_2 SA, had a shorter pulse duration and wider spectral width. The details can be seen in Table 1. The broad optical spectrum is due to the thin waist diameter of the fiber-taper WS_2 SA. A thinner waist diameter of the tapered fiber means a stronger non-linear effect. At this time, the strong non-linearity is conducive to the spectral broadening. Thus, the 3 dB spectral width becomes wider. In addition, the contrast studies on WS_2 SA, SWCNT SA and graphene SA have been presented in Table 2. Thus, it is important to make a tapered fiber with a smaller waist diameter and longer fused zone, and make fiber-taper WS_2 SA with large modulation depth.

4 Conclusion

In conclusion, a fiber-taper WS_2 SA with excellent performance has been prepared with 17.2% modulation depth, 34.02 MW cm^{-2} saturation intensity, and 59.5% non-saturable loss. In order to prevent the fiber from being broken and avoid oxidation and corrosion by the environment, a gold film has also been deposited on the surface of the fiber-taper WS_2 SAs. Using the prepared fiber-taper WS_2 SA with evanescent wave interaction, an all-fiber mode-locked EDF laser has been investigated experimentally. The maximum output power from OC is 18 mW at a pump power of 680 mW. 246 fs optical pulses

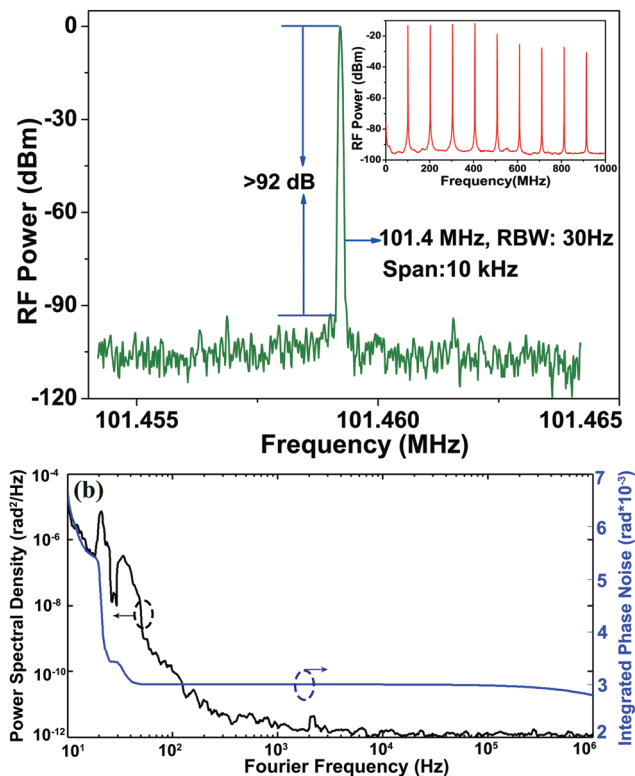


Fig. 4 (a) Radio frequency (RF) spectrum of the all-fiber mode-locked EDF laser based on the fiber-taper WS_2 SA. (b) The phase noise is measured at 101.4 MHz, and the timing jitter is 10 ps.

with a repetition rate of 101.4 MHz at 1561 nm have also been generated. To our best knowledge, these are the shortest pulses ever produced by all-fiber lasers based on TMD SAs. In addition, the 3 dB spectral width has been measured to be 57 nm, and the 92 dB RF spectrum has been obtained. We have calculated that the time jitter is 10 ps by integration from 1 MHz down to 10 Hz. The results in this paper demonstrated that the wider spectral width and shorter pulse duration of the mode-locked pulses can be obtained by using fiber-taper WS₂ SAs with a smaller waist diameter and longer fused zone of the tapered fiber, which can act as cost-effective photonic devices for ultrafast optics.

Acknowledgements

We express our sincere thanks to Peiguang Yan, Tuan Guo and Hao Chen for their valuable suggestions. This work has been supported by The National Key Basic Research Program of China (grant no. 2012CB821304, 2013CB922401, and 2013CB922402); National Natural Science Foundation of China (NSFC) (grant no. 11674036, 61378040, and 11078022); Fund of State Key Laboratory of Information Photonics and Optical Communications (Beijing University of Posts and Telecommunications, grant no. IPOC2016ZT04).

References

- 1 B. H. Chen, X. Y. Zhang, K. Wu, H. Wang, J. Wang and J. P. Chen, *Opt. Express*, 2015, **23**, 26723–26737.
- 2 G. Z. Wang, S. F. Zhang, X. Y. Zhang, L. Zhang, Y. Cheng, D. Fox, H. Z. Zhang, J. N. Coleman, W. J. Blau and J. Wang, *Photonics Res.*, 2015, **3**, A51–A55.
- 3 Z. Q. Luo, D. D. Wu, B. Xu, H. Y. Xu, Z. P. Cai, J. Peng, J. Weng, S. Xu, C. H. Zhu, F. Q. Wang, Z. P. Sun and H. Zhang, *Nanoscale*, 2016, **8**, 1066–1072.
- 4 R. I. Woodward and E. J. R. Kelleher, *Appl. Sci.*, 2015, **5**, 1440–1456.
- 5 S. F. Zhang, N. N. Dong, N. McEvoy, M. O'Brien, S. Winters, N. C. Berner, C. Yim, X. Y. Zhang, Z. H. Chen, L. Zhang, G. S. Duesberg and J. Wang, *ACS Nano*, 2015, **9**, 7142–7150.
- 6 X. Y. Zhang, S. F. Zhang, C. X. Chang, Y. Y. Feng, Y. X. Li, N. N. Dong, K. P. Wang, L. Zhang, W. J. Blau and J. Wang, *Nanoscale*, 2015, **7**, 2978–2986.
- 7 X. Y. Zhang, S. F. Zhang, B. H. Chen, H. Wang, K. Wu, Y. Chen, J. T. Fan, S. Qi, X. L. Cui, L. Zhang and J. Wang, *Nanoscale*, 2016, **8**, 431–439.
- 8 M. E. Fermann and I. Hart, *Nat. Photonics*, 2013, **7**, 868–874.
- 9 Z. Jiang, C. B. Huang, D. E. Leaird and A. M. Weiner, *Nat. Photonics*, 2007, **1**, 463–467.
- 10 F. Wang, A. G. Rozhin, V. Scardaci, Z. Sun, F. Hennrich, I. H. White, W. I. Milne and A. C. Ferrari, *Nat. Nanotechnol.*, 2008, **3**, 738–742.
- 11 J. Sotor, G. Sobon, M. Kowalczyk, W. Macherzynski, P. Paletko and K. M. Abramski, *Opt. Lett.*, 2015, **40**, 3885–3888.
- 12 D. Mao, B. B. Du, D. X. Yang, S. L. Zhang, Y. D. Wang, W. D. Zhang, X. Y. She, H. C. Cheng, H. B. Zeng and J. L. Zhao, *Small*, 2016, **12**, 1489–1497.
- 13 H. Chen, Y. S. Chen, J. D. Yin, X. J. Zhang, T. Guo and P. G. Yan, *Opt. Express*, 2016, **24**, 16287–16296.
- 14 P. G. Yan, A. J. Liu, Y. S. Chen, H. Chen, S. C. Ruan, C. Y. Guo, S. F. Chen, I. L. Li, H. P. Yang, J. G. Hu and G. Z. Cao, *Opt. Mater. Express*, 2015, **5**, 479–489.
- 15 W. J. Liu, L. H. Pang, H. N. Han, W. L. Tian, H. Chen, M. Lei, P. G. Yan and Z. Y. Wei, *Sci. Rep.*, 2016, **6**, 19997.
- 16 U. Keller, K. J. Weingarten, F. X. Kartner, D. Kopf, B. Braun, I. D. Jung, R. Fluck, C. Honninger, N. Matuschek and J. Aus der Au, *IEEE J. Sel. Top. Quantum Electron.*, 1996, **2**, 435–453.
- 17 A. A. Lagatsky, F. Fusari, S. Calvez, S. V. Kurilchik, V. E. Kisel, N. V. Kuleshov, M. D. Dawson, C. T. A. Brown and W. Sibbert, *Opt. Lett.*, 2010, **35**, 172–174.
- 18 Y. Nozaki, N. Nishizawa, E. Omoda, H. Kataura and Y. Sakakibara, *Opt. Lett.*, 2012, **37**, 5079–5081.
- 19 J. Sotor, G. Sobon, J. Jagiello, L. Lipinska and K. M. Abramski, *J. Appl. Phys.*, 2015, **117**, 133103.
- 20 H. Jeong, S. Y. Choi, F. Rotermund, Y. H. Cha, D. Y. Jeong and D. I. Yeom, *Opt. Express*, 2014, **22**, 22667–22672.
- 21 A. Martinez and Z. P. Sun, *Nat. Photonics*, 2013, **7**, 842–845.
- 22 H. Lee, W. S. Kwon, J. H. Kim, D. Kang and S. Kim, *Opt. Express*, 2015, **23**, 22116–22122.
- 23 J. W. Kim, S. Y. Choi, B. H. Jung, D. I. Yeom and F. Rotermund, *Appl. Phys. Express*, 2013, **6**, 032704.
- 24 Y. W. Song, S. Y. Jang, W. S. Han and M. K. Bae, *Appl. Phys. Lett.*, 2010, **96**, 051122.
- 25 G. Sobon, J. Sotor, I. Pasternak, A. Krajewska, W. Strupinski and K. M. Abramski, *Opt. Mater. Express*, 2015, **5**, 2884–2894.
- 26 Y. Chen, S. Chen, J. Liu, Y. Gao and W. Zhang, *Opt. Express*, 2016, **24**, 13316–13324.
- 27 D. Mao, X. She, B. Du, D. Yang, W. Zhang, K. Song, X. Cui, B. Jiang, T. Peng and J. Zhao, *Sci. Rep.*, 2016, **6**, 23583.
- 28 R. I. Woodward, R. C. T. Howe, G. Hu, F. Torrisi, M. Zhang, T. Hasan and E. J. R. Kelleher, *Photonics Res.*, 2015, **3**, A30–A42.
- 29 Z. Q. Luo, Y. Y. Li, M. Zhong, Y. Z. Huang, X. J. Wan, J. Peng and J. Weng, *Photonics Res.*, 2015, **3**, A79–A86.
- 30 F. Lou, R. W. Zhao, J. L. He, Z. T. Jia, X. C. Su, Z. W. Wang, J. Hou and B. T. Zhang, *Photonics Res.*, 2015, **3**, A25–A29.
- 31 H. D. Xia, H. P. Li, C. Y. Lan, C. Li, J. B. Du, S. J. Zhang and Y. Liu, *Photonics Res.*, 2015, **3**, A92–A96.
- 32 C. Cheng, H. L. Liu, Z. Shang, W. J. Nie, Y. Tan, B. R. Rabes, J. R. V. Aldana, D. Jaque and F. Chen, *Opt. Mater. Express*, 2016, **6**, 367–373.
- 33 R. F. Wei, H. Zhang, X. L. Tian, T. Qiao, Z. L. Hu, Z. Chen, X. He, Y. Z. Yu and J. R. Qiu, *Nanoscale*, 2016, **8**, 7704–7710.
- 34 Z. Tian, K. Wu, L. C. Kong, N. Yang, Y. Wang, R. Chen, W. S. Hu, J. Q. Xu and Y. L. Tang, *Laser Phys. Lett.*, 2015, **12**, 065104.

- 35 S. W. Wang, Y. Zhou, Y. Wang, S. Yan, Y. Li, W. G. Zheng, Y. Deng, Q. H. Zhu, J. Q. Xu and Y. L. Tang, *Laser Phys. Lett.*, 2016, **13**, 055102.
- 36 K. Wu, X. Y. Zhang, J. Wang and J. P. Chen, *Opt. Lett.*, 2015, **40**, 1374–1377.
- 37 A. P. Luo, M. Liu, X. D. Wang, Q. Y. Ning, W. C. Xu and Z. C. Luo, *Photonics Res.*, 2015, **3**, A69–A78.
- 38 H. Ahmad, Z. C. Tiu, A. Zarei, M. Suthaskumar, M. A. M. Salim and S. W. Harun, *Appl. Phys. B*, 2016, **122**, 69.
- 39 K. Wu, X. Y. Zhang, J. Wang, X. Li and J. P. Chen, *Opt. Express*, 2015, **23**, 11453–11461.
- 40 D. Mao, S. Zhang, Y. Wang, X. Gan, W. Zhang, T. Mei, Y. Wang, Y. Wang, H. Zeng and J. Zhao, *Opt. Express*, 2015, **23**, 27509–27519.
- 41 M. Jung, J. Lee, J. Park, J. Koo, Y. M. Jhon and J. H. Lee, *Opt. Express*, 2015, **23**, 19996–20006.
- 42 H. Guoyu, Y. Song, K. Li, Z. Dou, J. Tian and X. Zhang, *Laser Phys. Lett.*, 2015, **12**, 125102.
- 43 B. Guo, Y. Yao, P. G. Yan, K. Xu, J. J. Liu, S. G. Wang and Y. Li, *IEEE Photonics Technol. Lett.*, 2016, **28**, 323–326.
- 44 R. Khazaeinezhad, S. H. Kassani, H. Jeong, D. Yeom and K. Oh, *J. Lightwave Technol.*, 2015, **33**, 3550–3557.
- 45 R. Khazaeinezhad, S. H. Kassani, H. Jeong, K. J. Park, B. Y. Kim, D. Yeom and K. Oh, *IEEE Photonics Technol. Lett.*, 2015, **27**, 1581–1584.
- 46 J. Lin, Y. Y. Hu, C. J. Chen, C. Gu and L. X. Xu, *Opt. Express*, 2015, **23**, 29059–29064.
- 47 S. H. Kassani, R. Khazaeinezhad, H. Jeong, T. Nazari, D. Yeom and K. Oh, *Opt. Mater. Express*, 2015, **5**, 373–379.
- 48 L. H. Pang, W. J. Liu, W. L. Tian, H. N. Han and Z. Y. Wei, *IEEE Photonics J.*, 2016, **8**, 1501907.
- 49 W. J. Liu, L. H. Pang, H. N. Han, Z. W. Shen, M. Lei, H. Teng and Z. Y. Wei, *Photonics Res.*, 2016, **4**, 111–114.
- 50 W. S. Kwon, H. Lee, J. H. Kim, J. Choi, K. S. Kim and S. Kim, *Opt. Express*, 2015, **23**, 7779–7785.
- 51 J. Sotor, I. Pasternak, A. Krajewska, W. Strupinski and G. Sobon, *Opt. Express*, 2015, **23**, 27503–27508.
- 52 S. Ko, J. Lee, J. Koo, B. S. Joo, M. Gu and J. H. Lee, *J. Lightwave Technol.*, 2016, **34**, 3776–3784.
- 53 N. H. Park, H. Jeong, S. Y. Choi, M. H. Kim, F. Rotermund and D. Yeom, *Opt. Express*, 2015, **23**, 19806–19812.
- 54 H. Jeong, S. Y. Choi, M. H. Kim, F. Rotermund, Y. H. Cha, D. Y. Jeong, S. B. Lee, K. Lee and D. Yeom, *Opt. Express*, 2016, **24**, 14152–14158.
- 55 K. Park, J. Lee, Y. T. Lee, W. K. Choi, J. H. Lee and Y. W. Song, *Ann. Phys.*, 2015, **527**, 770–776.
- 56 W. Li, B. Chen, C. Meng, W. Fang, Y. Xiao, X. Li, Z. Hu, Y. Xu, L. Tong, H. Wang, W. Liu, J. Bao and Y. R. Shen, *Nano Lett.*, 2014, **14**, 955–959.